

Towards antituberculosis drugs: virtual screening for potential inhibitors of pantothenate synthetase of *Mycobacterium tuberculosis*

By Vivien Cherie C. Uy and Junie B. Billones*

Department of Physical Sciences and Mathematics, College of Arts and Sciences University of the Philippines Manila, Padre Faura, Ermita, Manila 1000 Philippines

A structure-based pharmacophore has been generated based on the binding site of pantothenate synthetase. The pharmacophore was used to screen libraries of compounds for potential inhibitors of the enzyme. The top hit was compound NSC_125296 (2-hydroxy-3-[(2E)-1-(3-hydroxy-1,4-dioxonaphthalen-2-yl)-3-phenylprop-2-en-1-yl]naphthalene-1,4-dione) with binding energy that is over three times better than that of a known inhibitor nafrotyl oxalate. Subsequent structural modification of NSC_125296 yielded compounds with better binding energies compared to that of native substrate pantoyl adenylate.

*Corresponding author

Email Address: jbillones@upm.edu.ph

Submitted: June 7, 2012

Revised: July 4, 2012

Accepted: July 7, 2012

Published: August 27, 2012

Editor-in-charge: Gisela P. Padilla - Concepcion

Reviewers:

Baltazar D. Aguda

Len Herald V. Lim

KEYWORDS

Tuberculosis, pantothenate synthetase, structure-based pharmacophore, virtual screening, molecular docking

INTRODUCTION

Tuberculosis (TB), a disease caused by the infection of *Mycobacterium tuberculosis* (MTB), has infected more than one third of the world's population (Corbett et al. 2003). The World Health Organization (WHO) estimated that about 9.4 million TB cases emerged in 2009 including 1.1 million cases among people with HIV. TB caused 0.38 million deaths among HIV-positive people and 1.3 million deaths among those who are negative of HIV (WHO 2010/2011). The current treatment of TB involves primarily the use of Isoniazid and Rifampicin and other first-line drugs such as Streptomycin, Pyrazinamide, and Ethambutol (Varaine et al. 2010). Unfortunately, the use of these drugs also led to an increased number of resistant strains (Johnson et al. 2006). Resistance may arise from the non-compliance in the usage of drugs in either taking less than the prescribed dose or taking only one of the combination drugs (Davies 1999). The misuse of TB drugs results to resistance to first-line drugs known as multi-drug resistant tuberculosis (MDR-TB) and extensively drug resistant tuberculosis (XDR-TB), which is defined as

MDR-TB with additional resistance to second-line anti-TB drugs such as fluoroquinolones and at least one of the injectables (WHO 2010/2011, Shah et al. 2007, Van Rie and Enarson 2006).

The ability of MTB to persist by not actively growing and having its overall metabolic activity down-regulated, often termed nonreplicating persistence (NRP), renders the available drugs ineffective against NRP-MTB. Consequently, a minimum of 6 months of treatment has been required to prevent relapse. It is therefore imperative to discover and develop compounds against NRP-MTB.

One attractive target for MTB inhibition is pantothenate synthetase (PS), an enzyme that catalyzes the condensation of

pantothenate (Vitamin B5) from D-pantoate and β -alanine (Zheng and Blanchard 2001). Pantothenate is important in bacteria because it is necessary for the biosynthesis of Coenzyme A (CoA) and Acyl Carrier Protein (ACP). Humans, unlike bacteria, do not have the PS enzyme, thus they obtain Vitamin B5 through the diet. Because the enzyme is not present in humans, PS is a good target for drugs against TB (White et al. 2007). In fact, several publications in recent past are focused on this enzyme as potential antimicrobial target (Tuck et al. 2006, Southworth et al. 2007, Velaparthy et al. 2008, Ciulli et al. 2008, Hung et al. 2009, Yang et al. 2011).

In this study, we performed a virtual screening of over 300,000 synthetic and natural compounds based on the pharmacophore generated from the crystal structure of pantothenate synthetase (PDB: 1N2H) (Wang and Eisenberg 2003). Further modification of the lead compound resulted in the identification of several structures with greater binding energies than the natural intermediate, pantoyl adenylate, and a known inhibitor, nafronyl oxalate.

METHODOLOGY

All computational methods were done using Discovery Studio (DS) 2.5.5 (Accelrys, Inc). The pdb file (1N2H) for the crystal structure of pantothenate synthetase in complex with pantoyl adenylate from *M. tuberculosis* was obtained from RCSB Protein Data Bank (<http://www.rcsb.org/pdb/explore.do?structureId=1n2h>). The protein was then cleaned, prepared, and optimized using CHARMM (Chemistry at HARvard Macromolecular Mechanics) forcefield (Brooks et al. 1983, Brooks et al. 2009). Cleaning involved removal of water molecules and ions while protein preparation allowed addition of missing atoms and introduction of appropriate charges (e.g. protonation of amino groups and deprotonation of carboxylic functionality) on residues at physiological condition. Geometry optimization involved variation of atomic coordinates and searching for the lowest-energy conformation. The CHARMM forcefield used in this work, like the other molecular mechanics forcefields, includes energy components associated with bond stretching, bending, torsion, and non-bonding interactions in calculating the energy of the molecule. Finally, since PS is a homodimer only domain A was used in the computational processes.

The compound libraries NCI-Open_09-03 (260,071), Complete Screening January 2011 (42,709), TOSLab_Collection (16,657), Hitfinder_V10 (14,400), and NATx_Release_100915_All_20674_cpds (20,674), were obtained as SDF from NCI (<http://cactus.nci.nih.gov/download/nci/>), Keyorganics (<http://www.keyorganics.co.uk/Downloads>), Toslab (http://www.toslab.com/Products_Services/Collection_of_Compounds/collection.htm), Maybridge (http://www.maybridge.com/portal/alias_Rainbow/lang_en-US/tabID_229/DesktopDefault.aspx), and AnalytiCon-

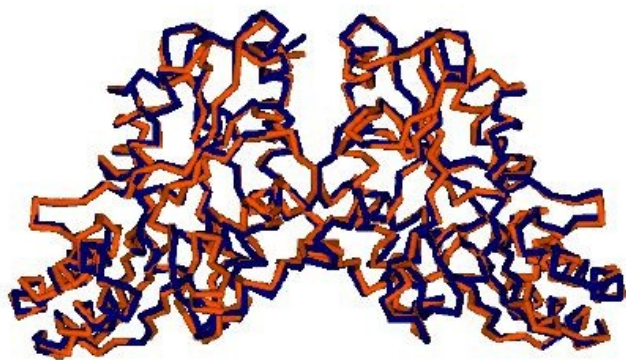


Figure 1. Superimposition of original (blue) and prepared (orange) pantothenate synthetase structures. RMSD is 0.81 Å.

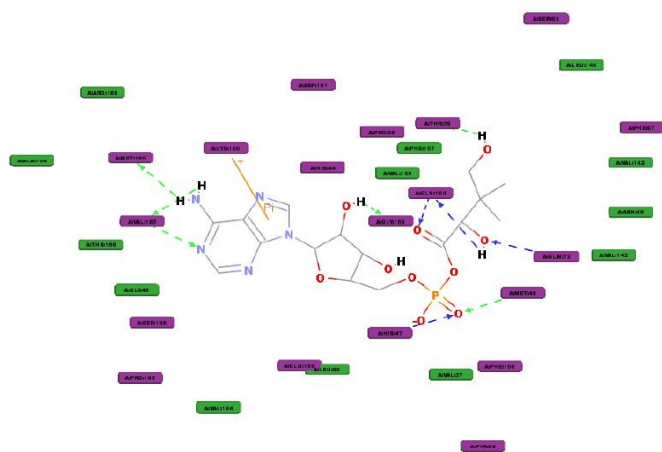


Figure 2. Interaction diagram for pantothenate synthetase – pantoyl adenylate complex. Violet residues have polar interactions; green residues have van der Waals interactions; dashed blue and green lines indicate H-bonding interactions; and orange line represents pi interaction.

Discovery (<http://www.ac-discovery.com/>), respectively. The compounds were then prepared allowing ionization, generation of tautomers and isomers, and application of Lipinski Filter. Then a database of 3D structures was built consisting of the library compounds and their isomers.

For the first screening, a rigid fitting method was used by which the ligands were docked to the binding site of the receptor using shape-based searching algorithm. Specifically, rapid rigid body docking was performed with the well-known ZDOCK algorithm (Pierce and Weng 2008, Chen and Weng 2003), which employs a fast Fourier Transform-based search algorithm using a pair-wise shape complementarity function for identifying docked conformations. The docked structures were scored based on atomic contact energies. After exhaustive search in the translational and rotational space a subsequent refining algorithm, ZRANK (Pierce and Weng 2007), was employed for structure refinement and re-ranking. The RDOCK algorithm (Li et al. 2003) was used to refine ZDOCK hits based on a CHARMM energy minimization and poses were scored by CHARMM energy and desolvation energy.

To trim down the number of compounds, only those with fit values above 3.35 were considered for the second screening. These compounds were screened using flexible fitting method. Flexible docking combines the strength of CHARMM for accurate receptor sampling with effective, features-based docking (Koska et al. 2008). DS Flexible Docking is a practical approach to flexible docking in which the docking of small molecules is influenced by prevailing low-energy conformations of side chains in the active site (Accelrys Inc.). The compounds with fit values above 4.0 were subsequently docked to the enzyme using CDOCKER protocol and employing the CHARMM forcefield. The CDOCKER algorithm is a grid-based molecular docking method (Wu et al. 2003) that employs CHARMM forcefield. With CDOCKER, initial ligand conformations are sampled via high temperature molecular dynamics and are also allowed to flex during the refinement through simulated annealing. CDOCKER has been shown to give highly accurate docked poses (Erickson et al 2004).

RESULTS AND DISCUSSION

The superimposition of the original and model enzyme (Figure 1) gave an RMSD of 0.81 Å, which is well within the acceptable range (Dias and de Azevedo 2008), and indicated that there was no significant alteration in the overall structure of PS during target enzyme preparation. With this enzyme model at hand, we carried out molecular docking of the natural substrate pantoyl adenylate (PA), known inhibitor nafronyl oxalate, and the top hits obtained from virtual high throughput screening.

The actual biological activity of a compound is the sum of all factors associated with the delivery of the compound to the receptor and the close-range interaction of the compound with

the relevant residues in the active site. Molecular docking addresses the latter while the application of Lipinski filter during virtual screening eliminates the compounds that do not meet the Lipinski's criteria (*i.e.* H-bond donors ≤ 5 , H-bond acceptors ≤ 10 , MM < 500, logP ≤ 5 , compound classes that are substrates for biological transporters are exceptions to the rule) of drug likeness (Lipinski 2001). In docking it is assumed that the docked ligand has already overcome all obstacles (e.g. solubility, absorption, solvent interaction, etc.) along the way to reach the target site. Although our docking protocol does not consider solvent molecules explicitly, its scoring function combines both CHARMM energy and desolvation energy. Moreover, the use of enzyme model based on the crystal structure takes into account the effect of the aqueous environment in achieving the final conformation of the receptor.

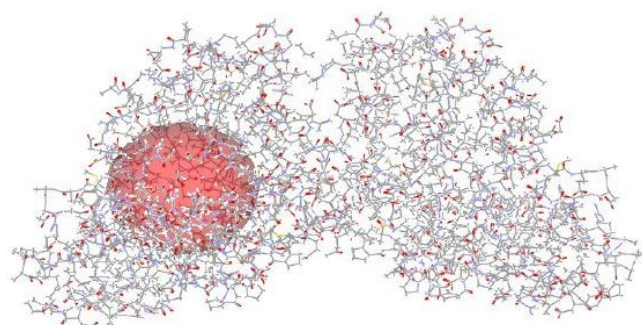


Figure 3. The 3D structure of pantothenate synthetase and the defined site sphere (red) encompassing the active site.

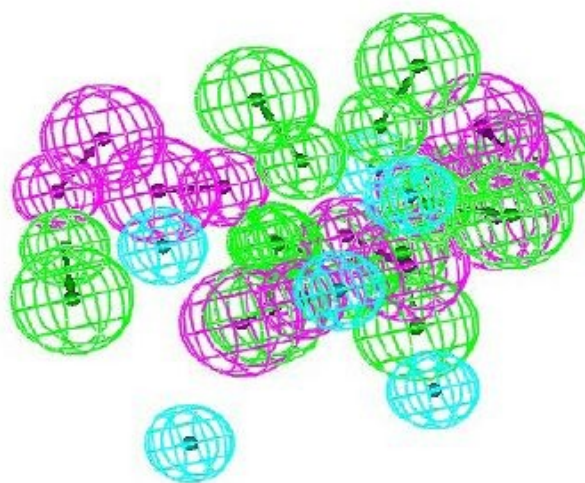


Figure 4. Generated clustered pharmacophore. It is composed of 20 features: acceptor (green), donor (violet) and hydrophobe (blue)

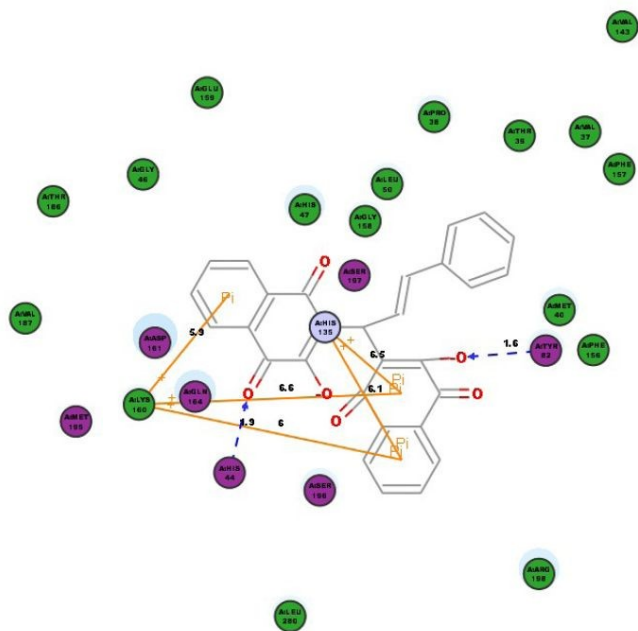


Figure 5. Interaction diagram for NSC_125296 – PS complex. Violet residues have polar interactions; green residues have van der Waals interactions; dashed blue lines indicate Hbonding interactions; and orange line represents pi interaction.

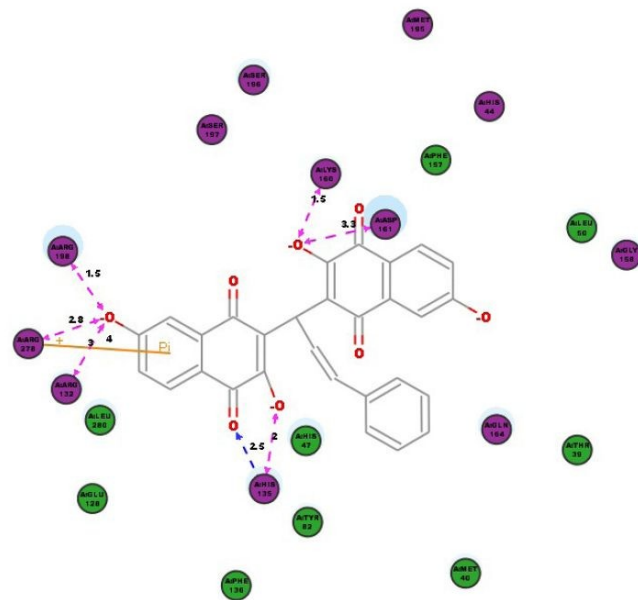


Figure 6. Interaction diagram for compound 1 with PS enzyme. Violet residues have polar interactions; green residues have van der Waals interactions; dashed blue line indicate H-bonding interaction; pink line is charged interaction, and orange line represents pi interaction.

The interaction of PA with the model enzyme (Figure 2) was performed in order to validate the docking protocol employed in this work. The results of docking PA to the model PS were very similar to the interaction involving the native enzyme (Wang and Eisenberg 2003). In particular, PA interacts with the following residues in the active site: Pro38, Thr39, Met40, His44, Gly46, His47, Leu50, Asn69, Gln72, Tyr82, Val139, Val142, Val143, Phe157, Gly158, Lys160, Asp161, Gln164, Pro185, Thr186, Val187, and Met195. In fact, Zheng and coworkers observed that changing His44, His 47, Asn69, Gln72, Lys160, or Gln164 into alanine resulted in a decrease in PS activity (Zheng and Blanchard 2001), verifying the crucial role of the abovementioned residues.

The interaction diagram (Figure 2) shows that PA interacts by H-bonding with His47 and Met40 through its phosphate linker; with Thr39, Gln64 and Gln72 through its pantoyl moiety; and with Gly158, Val187, and Met195 through its adenine component. Additionally, a pi interaction was also formed with Lys160. The interactions with the rest of the identified residues were hydrophobic in character. Collectively, these observations are not only in accord with experiment, but the results also provide better understanding of the nature of interaction that PS makes with its ligands.

Having established the applicability of our docking protocol, we subsequently defined the site sphere in the enzyme within which we generated the pharmacophore. The pantoyl adenylate bound in domain A of PS was used to determine the site sphere. The generated site sphere, shown in Figure 3, has a radius of 10.6151Å and is assumed to cover the entire active site of the enzyme.

On the basis of the structural features embodied in the defined site sphere within the enzyme, a pharmacophore was generated using the *Interaction Generation* protocol in DS Catalyst. The *Interaction Generation* protocol takes the input receptor and a defined active site and analyzed the site for donors, acceptors, and hydrophobes. The utility of the Catalyst program in generating realistic pharmacophore has been documented in the recent past. DS Catalyst SBP (structure based pharmacophore) was instrumental in the identification of six compounds (from a quarter million of library compounds) that exhibited human cancer LNCaP proliferation inhibitory activities (Purushottamachar et al. 2007) and five compounds from NCI database that exhibited nanomolar activity against human protein tyrosine phosphatase (h-PTP 1B) inhibitors (Taha 2007).

The generated pharmacophore, which encompasses a hundred features was trimmed using *Cluster Current Feature* and *Keep Only Cluster Centers* tools in DS. The *Cluster Current Feature* performs a hierarchical clustering of the current feature and locates cluster centers of the feature groups. The *Keep Only Cluster Centers* deletes all non-center clusters. The final pharmacophore obtained was a combination of 20 features

involving acceptor, donor and hydrophobe characteristics (Figure 4). This pharmacophore was used to screen the databases for lead compounds against PS. The compounds with favorable fit values and passed the screening criteria were docked to the enzyme.

The fit values and binding energy of top five hits are displayed in Table 1. Except compound ER748740 (2-({4-hydroxy-5-[(4-methoxyphenyl)methyl]-6-oxo-1,6-dihydropyrimidin-2-yl}sulfanyl)-N-(4-methylphenyl)acetamide) from TOSLab, four out of five top hits came from National Cancer Institute (NCI) database namely: NSC_125296 (2-hydroxy-3-[(2E)-1-(3-hydroxy-1,4-dioxo-1,4-dihydronaphthalen-2-yl)-3-phenylprop-2-en-1-yl]-1,4-dihydronaphthalene-1,4-dione), NSC_167356 (2,4,4-trimethyl-4-[(N-[(4-methylbenzene)sulfonyl]hydrazinecarbonyl)butanoic acid), NSC_144248 (2-[N-(4-{[(4-methylbenzene)sulfonyl]oxy}phenyl)(4-methylbenzene)sulfonamido]acetic acid), and NSC_618496 (N'-[(1E)-1-(4-hydroxy-6-methyl-2-oxo-2H-pyran-3-yl)ethylidene]-4-methylbenzene-1-sulfonylhydrazide).

The results showed that the natural substrate pantoyl adenylate, having the most negative binding energy (BE = -482 kcal/mol), remained the best ligand among the compounds screened. Interestingly, the known inhibitor nafronyl oxalate displayed weaker binding interaction, as indicated by its binding energy (-98.5 kcal/mol) which is less negative by at least 100 kcal/mol compared with the top five hits. Moreover, among several hundred thousand compounds screened here, NSC_125296 gave relatively the highest binding energy (-356.418 kcal/mol). Therefore, this compound can be considered as an important lead in search for anti-TB drug.

In order to gain some insights on

Table 1. Rigid and Flexible Fit Values, and Binding Energies of top hits in virtual screening of PS inhibitors.

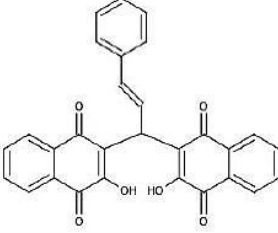
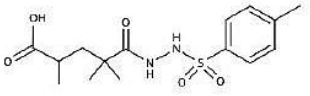
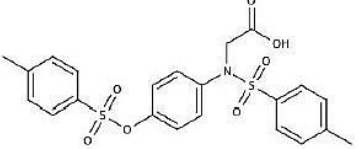
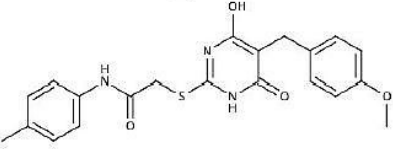
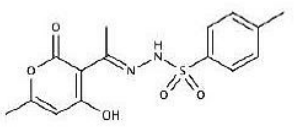
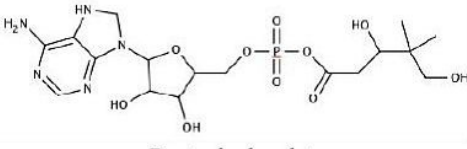
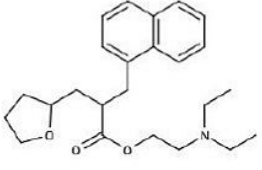
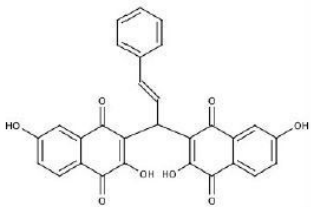
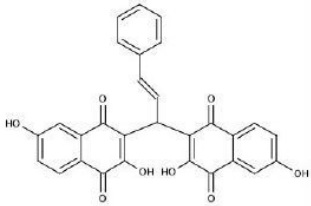
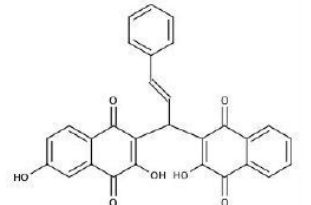
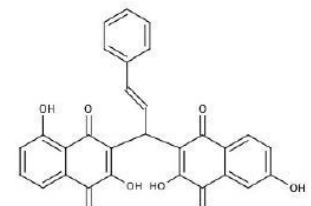
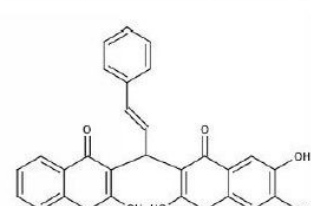
Compound	Fit Value (Rigid)	Fit Value (Flexible)	Binding Energy (kcal/mol)
 NSC_125296	3.37	4.12	-356.42
 NSC_167356	3.77	4.26	-301.93
 NSC_144248	3.39	4.08	-287.81
 ER748740	3.35	4.05	-252.08
 NSC_618496	4.04	4.33	-221.87
 Pantoyl adenylate	2.76	3.31	-482.00
 Nafronyl oxalate	--	--	-98.58

Table 2. Type and number of interactions for the top five hits including pantoyl adenylate (PA) and nafronyl oxalate (NO) with pantothenate synthetase (PS).

Compound	Polar	Hydrophobic	H-Bond	Charged	Pi
NSC_125296	7	17	2	0	5
NSC_167356	6	10	4	2	1
NSC_144248	9	10	2	2	2
ER748740	9	12	5	0	0
NSC_618496	7	10	2	2	0
PA	11	11	10	0	1
NO	6	20	0	0	0

Table 3. Binding Energy for Docking the Derivatives of NSC_125296 with PS.

Compound	Structure	Binding Energy (kcal/mol)
1		-721.76
2		-712.79
3		-706.23
4		-649.47
5		-488.07

the structural requirements for PS inhibition, we examined the interaction of PS with the identified leads. Thus, the count and type of interaction present between PS and the lead compounds were determined and the results are detailed in Table 2.

The strength of the interactions between the enzyme and the ligand, as measured by the binding energy, is the summation of attractive and repulsive interactions including polar, van der Waals, H-bonding, charged, and pi interactions. Accordingly, the very strong interaction of PS with pantoyl adenylate can be attributed to the remarkably high number of H-bonds formed (*vide supra*). Furthermore, PA showed the most number of polar interactions. On the other extreme, nafronyl oxalate makes no H-bond and has no charged and pi interactions with PS. In addition to a handful of polar interactions, it binds with the enzyme through hydrophobic interactions only. These explain the relatively low binding energy of NO. Nevertheless, the interaction of NO with the catalytic residues explains its ability to bind with PS. Although in reality NO forms long-range H-bonding with His44 and His47, the parameters used in this work were such that H-bonding in that range cannot be recognized.

On the other hand, the top hit NSC_125296 interacted with PS in an uncommon fashion (Figure 5). Amazingly, the distinct binding energy of this compound cannot be attributed to the number of H-bonds but to atypical cation-pi interactions. Lys160 formed cation-pi interactions with the three aromatic rings of NSC_125296, while His135 interacted in the same manner with a naphthalenyl moiety. Cation-pi interactions are unusually strong and are considered to be as strong as H-bonding interactions. Thus, despite having only a couple of H-bonds, the binding energy of NSC_125296 was

Table 4. Type and number of interactions for compounds derived from NSC_125296 with PS enzyme.

Compound	Polar	Hydrophobic	H-Bond	Charged	Pi
1	12	9	1	6	1
2	14	10	1	8	4
3	11	12	1	5	0
4	14	9	3	6	2
5	10	10	4	2	2

relatively high because of the notably numerous cation-pi interactions. In addition to these, there were almost as many polar and hydrophobic interactions in NSC_125296 as there were in NO. Specifically, NSC_125296 formed H-bonding interactions with His44 and Tyr82, polar interactions with His44, Tyr82, Asp161, Gln164, Met195, Ser196, and Ser197, and van der Waals interactions with Val37, Pro38, Thr39, Met40, Gly46, His47, Leu50, Val143, Phe156, Phe157, Gly158, Glu159, Lys160, Thr186, Val187, Arg198, and Leu280.

Meanwhile, the interaction diagrams for NSC_167356, NSC_144248, ER748740 and NSC_618496 displayed similar number and type of interactions and thus clearly explain the comparable binding energies of these compounds. Moreover, these compounds interacted with a common set of residues namely: Thr39, Met40, His44, His47, Leu50, Lys160, Asp161, Gln164, Met195, and His135.

In our desire to find novel compounds with comparable, if not better, binding affinity with PS, we modified the structure of the lead compound NSC_125296 by arbitrarily varying the number and position of hydroxyl groups in the naphthalenyl moiety. Fortunately, we obtained five derivatives of the lead compound that afforded binding energy values far better than the natural substrate pantoate (Table 3).

Among the variants of NSC_125296, **1** (3-[(2E)-1-(3,7-dihydroxy-1,4-dioxo-1,4-dihydronaphthalen-2-yl)-3-phenylprop-2-en-1-yl]-2,6-dihydroxy-1,4-dihydronaphthalene-1,4-dione) provided the highest binding energy of -721.76 kcal/mol. It was closely followed by **2** (3-[(2E)-1-(3,6-dihydroxy-1,4-dioxo-1,4-dihydronaphthalen-2-yl)-3-phenylprop-2-en-1-yl]-2,6-dihydroxy-1,4-dihydronaphthalene-1,4-dione), **3** (3,6-dihydroxy-2-[(2E)-1-(3-hydroxy-1,4-dioxo-1,4-dihydronaphthalen-2-yl)-3-phenylprop-2-en-1-yl]-1,4-dihydronaphthalene-1,4-dione) and **4** (3-[(2E)-1-(3,6-dihydroxy-1,4-dioxo-1,4-dihydronaphthalen-2-yl)-3-phenylprop-2-en-1-yl]-2,5-dihydroxy-1,4-dihydronaphthalene-1,4-dione). However, compound **5** (2,6,7-trihydroxy-3-[(2E)-1-(3-hydroxy-1,4-dioxo-1,4-dihydronaphthalen-2-yl)-3-phenylprop-2-en-1-yl]-1,4-dihydronaphthalene-1,4-dione), gave a binding energy of -488.07 kcal/mol, which is very close to the

binding energy of PA.

Examination of the interaction diagrams for these compounds and Tables 3 and 4 revealed that simple addition of one or two hydroxyl groups resulted in a remarkable increase in number of charged interactions. For example, in compound **1** the extra OH group at C-7 in each naphthalenyl moiety caused the formation of additional five polar and six charged interactions, albeit the hydrophobic interactions were greatly reduced (Figure 6). Compound **1** had polar interactions with His44, Arg132, His135, Gly158, Lys160, Asp161, Gln164, Met195, Ser196, Ser197, Arg198, and Arg278, and van der Waals interactions with Thr39, Met40, His47, Leu50, Tyr82, Glu128, Phe137, Leu280, and Phe157. Furthermore, it formed an H-bond with His135, an interaction not found with the parent molecule, NSC_125296. It is noteworthy that the cation-pi interactions in the original lead compound were almost totally non-existent and were replaced by significantly stronger charged interactions. The interaction diagrams for the other compounds (**2** – **5**) did not appear very differently from one another in terms of number and type of interactions. In general, the extra hydroxyl groups in the structure of the lead compound fortified the interactions with pantothenate synthetase through the formation of additional polar and charged interactions especially with Arg132, Arg198, and Arg298 residues, which were also featured in previous experimental studies (Wang and Eisenberg 2003, von Delft et al 2001).

CONCLUDING REMARKS

The structure of pantothenate synthetase from *Mycobacterium tuberculosis* has been modeled and a pharmacophore was subsequently generated based on the structure of the active site of the enzyme. The pharmacophore, consisting of clustered acceptor, donor, and hydrophobe features, was used in screening several libraries of some 300,000 compounds encompassing both synthetic entities and natural products. The virtual screening efforts afforded five compounds with binding energies far better than that of known inhibitor, nafronyl oxalate. Among the library compounds, compound NSC_125296 (2-hydroxy-3-[(2E)-1-(3-hydroxy-1,4-dioxo-1,4-

dihydronaphthalen-2-yl)- 3-phenylprop-2-en-1-yl]- 1,4-dihydronaphthalene-1,4-dione) from NCI database gave the best (most negative) binding energy, albeit this is slightly lower than that of the native substrate pantoyl adenylate. The high affinity of NSC_125296 was found to be due to several unusual cation- π interactions involving Lys160 and His135 residues. Elaboration of the top most lead compound NSC_125296 by simple variation of the number and position of hydroxyl groups in the naphthalenyl moieties yielded five compounds which have binding energies significantly greater than that of the native reaction intermediate pantoyl adenylate. The high binding energy of the NSC_125296 variants are attributed to the remarkable increase in the number of polar and charged interactions and the positioning of the hydroxyl group in a way that allows charged interactions with Arg132, Arg198, and Arg298 catalytic residues.

The promising results of this theoretical study may elicit interest on the synthetic preparation of NSC_125296 derivatives as antitubercular compounds and the corresponding experimental evaluation of their antimycobacterial activity. Finally, this work provides distinct access to a novel class of compounds with anti-tuberculosis activity and hopefully leads to the ultimate goal – a new antituberculosis drug.

ACKNOWLEDGEMENT

We are grateful to Accelrys, Inc. (Singapore) for the Discovery Studio software.

CONFLICTS OF INTEREST

None

CONTRIBUTION OF INDIVIDUAL AUTHORS

VCCU performed the computational work under the supervision of JBB.

JBB developed the idea of this study and prepared the final manuscript.

REFERENCES

Accelrys Inc. Datasheet: Discovery Studio science portfolio. Retrieved from www.accelrys.com/products/datasheets/discovery-studio-overview.pdf

Brooks BR, Bruccoleri RE, Olafson BD, States DJ, Swaminathan S, Karplus M. CHARMM: a program for macromolecular energy, minimization, and dynamics calculations. *J. Comp. Chem.* 1983; 4: 187-217.

Brooks BR, Brooks III CL, Mackerell AD, Nilsson L, Petrella RJ, Roux B, Won Y, Archontis G, Bartels C, Boresch S, Caflisch A, Caves L, Cui Q, Dinner A. R, Feig M, Fischer S, Gao J, Hodoscek M, Im W, Kuczera K,

Lazaridis T, Ma J, Ovchinnikov V, Paci E, Pastor RW, Post CB, Pu JZ, Schaefer M, Tidor B, Venable RM, Woodcock HL, Wu X, Yang W, York DM, Karplus M. CHARMM: the biomolecular simulation program, *J. Comp. Chem.* 2009; 30: 1545-1615.

Chen R, Weng Z. ZDOCK: an initial-stage protein-docking algorithm. *Proteins* 2003, 52, 80-87.

Ciulli A, Scott DE, Ando M, Reyes F, Saldanha SA, Tuck KL, Chirgadze DY, Blundell TL, Abell C. Inhibition of *Mycobacterium tuberculosis* pantothenate synthetase by analogues of the reaction intermediate. *Chembiochem.* 2008; 9(16): 2606-11.

Corbett EL, Watt CJ, Walker N, Maher D, Williams BG, Raviglione M, Dye, C. The growing burden of tuberculosis: global trends and interactions with the HIV epidemic. *Arch. Intern. Med.* 2003; 163: 1009–21.

Davies, PDO. Multi-drug resistant tuberculosis. 1999. Retrieved from <http://priority.com/emol/TBMultiid.htm>.

Dias R, de Azevedo WF Jr., Molecular Docking Algorithms. *Current Drug Targets* 2008; 9: 1040-1047.

Erickson JA, Jalaie M, Robertson DH, Lewis RA, Vieth M. Lessons in molecular recognition: the effects of ligand and protein flexibility on molecular docking accuracy," *J Med Chem.* 2004, 47(1), 45-55.

Johnson R, Streicher EM, Louw, GE, Warren W, van Helden PD, Victor TC. Drug resistance in *Mycobacterium tuberculosis*. *Curr. Iss. Mol. Biol.* 2006; 8: 97-112.

Hung AW, Silvestre HL, Wen S, Ciulli A, Blundell TL, Abell C. Application of fragment growing and fragment linking to the discovery of inhibitors of *Mycobacterium tuberculosis* pantothenate synthetase. *Angew Chem Int Ed Engl.* 2009; 48(45): 8452-6.

Koska J, Spassov VZ, Maynard AJ, Yan L, Austin N, Flook P.K, Venkatachalam CM. Fully automated molecular mechanics based induced fit protein–ligand docking method. *J. Chem. Inf. Model.* 2008; 48(10): 1965–1973

Li L, Chen R, Weng Z. RDOCK: refinement of rigid-body protein docking predictions. *Proteins* 2003; 53: 693-707.

Lipinski CA, Lombardo F, Dominy BW, Feeney P. Experimental and computational approaches to estimate solubility and permeability in drug discovery and development settings. *Adv. Drug Deliv. Rev.* 2001; 46: 3 – 26.

Purushottamachar P, Khandelwal A, Chopra P, Maheshwari N, Gediya LK, Vasaitis TS, Bruno R, Clement OO, Njar VCO. First pharmacophore-based identification of androgen receptor down-regulating agents: discovery of potent anti-prostate cancer agents. *Bioorg Med Chem* 2007; 15: 3413 – 3421.

Pierce B, Weng Z. A combination of rescoring and refinement significantly improves protein docking performance. *Proteins* 2008; 72(1): 270-279.

Pierce B, Weng Z. ZRANK: reranking protein docking predictions with an optimized energy function. *Proteins* 2007; 67(4): 1078-1086.

Shah NS, Wright A, Bai GH. Worldwide emergence of

- extensively drug-resistant tuberculosis. *Emerging Infectious Diseases* 2007; 13(3): 380–387.
- Southworth K, Sneed B, Ross L, Cooley S, Sosa MI, Manouvakhova A, Rasmussen L, White EL, Anathan A, Fletcher TM III, Goldman RC, Goulding C, Eisenberg D. Identifying pantothenate synthetase inhibitors of *Mycobacterium tuberculosis* from a high throughput screen. Presented at the 13th Annual Conference of the Society for Biomolecular Sciences (SBS), Montreal, Canada, 2007.
- Taha MO, Bustanji Y, Al-Bakri AG, Yousef AM, Zalloum WA, Al-Masri IM, Atallah N. Discovery of new potent human protein tyrosine phosphatase inhibitors via pharmacophore and QSAR analysis followed by in silico screening. *J Mol Graph Model* 2007; 25(6): 870-84.
- Tuck KL, Saldanha SA, Birch LM, Smith AG, Abell C. The design and synthesis of inhibitors of pantothenate synthetase. *Org. Biomol. Chem.* 2006; 4: 3598–3610.
- Van Rie A, Enarson D. XDR tuberculosis: an indicator of public-health negligence. *The Lancet* 2006; 368(9547): 1554–1556.
- Varaine F, Henkens M, Gouzard V. (eds). *Tuberculosis*. (5th ed.). 2010. Retrieved from http://www.refbooks.msf.org/MSF_Docs/En/Tuberculosis/Tuberculosis_en.pdf.
- Velaparthi S, Brunsteiner M, Uddin R, Wan B, Franzblau SG, Petukhov PA. 5-*tert*-Butyl-*N*-pyrazol-4-yl-4,5,6,7-tetrahydrobenzo[*d*]isoxazole-3-carboxamide derivatives as novel potent inhibitors of *Mycobacterium tuberculosis* pantothenate synthetase: initiating a quest for new antitubercular drugs. *J. Med. Chem.* 2008; 51(7): 1999–2002.
- von Delft F, Lewendon A, Dhanaraj V, Blundell TL, Abell C, Smith AG. The crystal structure of *E. coli* pantothenate synthetase confirms it as a member of the cytidylyltransferase superfamily. *Structure* 2001; 9(5): 439-450.
- Wang S, Eisenberg D. Crystal structures of a pantothenate synthetase from *M. tuberculosis* and its complexes with substrates and a reaction intermediate. *Protein Science* 2003; 12: 1097–1108.
- White EL, Southworth K, Ross L, Cooley S, Gill RB, Sosa MI, Manouvakhova A, Rasmussen L, Goulding C, Eisenberg D, Fletcher TM. A novel inhibitor of *Mycobacterium tuberculosis* pantothenate synthetase. *Journal of Biomolecular Screening* 2007; 12: 100–105.
- WHO: 2010/2011 Tuberculosis Global Facts. Retrieved on from http://www.who.int/tb/publications/2010/factsheet_tb_2010.pdf.
- Wu, G, Robertson DH, Brooks CL III, Vieth M. Detailed analysis of grid-based molecular docking: a case study of CDOCKER - a CHARMM-based MD docking algorithm. *J Comp Chem* 2003; 24: 1549.
- Yang Y, Gao P, Liu Y, Ji X, Gan M, Guan Y, Hao X, Li Z, Xiao C. A discovery of novel *Mycobacterium tuberculosis* pantothenate synthetase inhibitors based on the molecular mechanism of actinomycin D inhibition. *Bioorg Med Chem Lett.* 2011; 21(13):3943-6.
- Zheng R, Blanchard JS. Steady-state and pre-steady-state kinetic analysis of *Mycobacterium tuberculosis* pantothenate synthetase. *Biochemistry* 2001; 40: 12904–12912.